Available online at www.sciencedirect.com
SCIENCE DIRECT®
International Journal of Thermal Sciences 42 (2003) 913–919
International Journal of Thermal Sciences
www.elsevier.com/locate/ijts

Development of an engineering approach to computations of turbulent flows in composite porous/fluid domains

A.V. Kuznetsov *, M. Xiong

Department of Mechanical and Aerospace Engineering, North Carolina State University, Campus Box 7910, Raleigh, NC 27695-7910, USA

Received 30 May 2002; accepted 6 December 2002

Abstract

The purpose of this paper is to develop an engineering approach to computations of turbulent flows in composite domains partly occupied by a clear fluid and partly by a fluid saturated porous medium. Previous research concerning turbulent flows in porous media indicates that the effect of porous media is to dampen turbulence. Therefore, in porous/fluid domains the penetration depth of turbulent eddies into the porous region is expected to be small. The authors suggest assuming that the flow over the whole porous region remains laminar and matching turbulent flow solution in the clear fluid region with the laminar flow solution in the turbulent flow region. Although the flow in the porous region is assumed to be laminar, linear Darcy or Brinkman–Darcy models cannot be utilized to describe momentum transport in the porous region because of large filtration velocity. The momentum transport model in the porous layer utilized in this research is based on the Brinkman–Forchheimer-extended Darcy equation, which allows the accounting for deviation from linearity and also allows a smooth matching of the filtration velocity at the porous/fluid interface. Because of the large filtration velocity in the porous region, the energy equation in the porous region also accounts for the thermal dispersion effects.

1. Introduction

Forced convection turbulent flow in composite porous/fluid domains is relevant to many industrial applications. Relevant examples include, but not limited to turbulent flows near porous obstacles [1] (this is an important problem, for example, in determining optimal parameters of tree shelterbelts), casting of binary alloys with electromagnetic stirring [2], avoiding freezing of gating channels in mould filling in casting processes, cooling of microelectronics [3], and modeling blood flow in partially closed coronary arteries because of the deposition of fatty material along their walls (this disease often requires a coronary artery bypass surgery). In general, this is a complicated problem and matching turbulent models for the clear fluid and porous regions is not trivial. However, in forced convection in composite porous/fluid domains most of the fluid flow is expected to go through the clear fluid region because of the considerable resistance that the porous layer creates to the flow. Recent theoretical and experimental investigations of turbulence in porous media (Antohe and Lage [4], Prakash et al. [5,6]) indicate is that the effect of porous media is to dampen turbulence, and this dampening is stronger for porous media of smaller permeability. It can be expected, therefore, that if the permeability of the porous layer is sufficiently small, the flow in the porous region will remain laminar even if the flow in the clear fluid region is turbulent. The whole porous region in this formulation becomes a large laminar sublayer. Indeed, true turbulence implies the existence of a cascade of energy from large eddies to smaller eddies. This cascade cannot develop in the porous region if permeability of the porous medium is sufficiently small.

Although the flow in the porous region is assumed laminar, it is expected that the dependence of flow velocity on the pressure gradient deviates from a linear correlation given by the Darcy law. This deviation can be accounted for by utilizing the Forchheimer extension of the Darcy law in the momentum equation and the thermal dispersion term in the energy equation (Nield and Bejan, [7]). It should be noted that there is a difference in opinions about the physical origin of the Forchheimer drag and thermal dispersion. Masuka and Takatsu [8] suggested that the Forchheimer flow resistance and thermal dispersion are caused mainly by turbulent mixing in porous media. A different point of view

* Corresponding author.
E-mail address: avkuznet@eos.ncsu.edu (A.V. Kuznetsov).

1290-0729/$ – see front matter
doi:10.1016/S1290-0729(03)00063-2

Nomenclature

a_f	fluid thermal diffusivity ..... $m^2 \cdot s^{-1}$
a_T	eddy diffusivity of heat ..... $m^2 \cdot s^{-1}$
A^+	Van Driest coefficient, defined in Eq. (17)
c_F	Forchheimer coefficient
C	dimensionless experimental constant in the correlation for thermal dispersion
d_p	average diameter of porous particle ..... m
Da	Darcy number, $= K/R^2$
F_{Kleb}	Klebanoff intermittency function, defined in Eq. (15)
h	heat transfer coefficient ..... $W \cdot m^{-2} \cdot K^{-1}$
k_f	fluid thermal conductivity ..... $W \cdot m^{-1} \cdot K^{-1}$
k_m	stagnant thermal conductivity of the porous medium ..... $W \cdot m^{-1} \cdot K^{-1}$
Nu	Nusselt number, $= h2R/k_f$
p	pressure ..... Pa
Pr	Prandtl number, $= \nu_f/a_f$
Pr_t	turbulent Prandtl number, $= \nu_T/a_T$
q''_W	wall heat flux ..... $W \cdot m^{-2}$
r	radial coordinate ..... m
r^+	dimensionless radial coordinate, $= u_\tau r/\nu_f$
R	duct radius ..... m
R^+	dimensionless radius of the tube, $= u_\tau R/\nu_f$
Re_p	Reynolds number based on the average particle diameter and the friction velocity at the porous/fluid interface, $= u_\tau d_p/\nu_f$
T	temperature ..... K
T_m	mean flow temperature ..... K
T_W	wall temperature ..... K
u	longitudinal velocity ..... $m \cdot s^{-1}$
u^+	dimensionless velocity, $= u/u_\tau$
u_τ	friction velocity at the porous/fluid interface, $= (\tau_i/\rho_f)^{1/2}$ ..... $m \cdot s^{-1}$
U_m^+	dimensionless mean flow velocity in the duct
y^+	dimensionless distance from the porous/fluid interface, $= \xi R^+ - r^+$
y_m^+	the smallest dimensionless distance from the interface for which $\mu_{T_i} = \mu_{T_o}$

Greek symbols

α_T	closure coefficient in the Cebeci–Smith model, defined in Eq. (17)
β	dimensionless adjustable coefficient in the matching condition for the shear stress at the porous/fluid interface
θ	dimensionless temperature for the constant wall heat flux case, $= (1/Nu)(T - T_W)/(T_m - T_W)$
κ	von Karman constant, defined in Eq. (17)
μ_{eff}	effective viscosity of porous medium ..... $kg \cdot m^{-1} \cdot s^{-1}$
μ_f	fluid viscosity ..... $kg \cdot m^{-1} \cdot s^{-1}$
μ_T	eddy viscosity ..... $kg \cdot m^{-1} \cdot s^{-1}$
μ_T^+	dimensionless eddy viscosity, $= \mu_T/\mu_f$
μ_{T_i}	dimensionless eddy viscosity in the inner layer
μ_{T_o}	dimensionless eddy viscosity in the outer layer
ν_f	fluid kinematic viscosity ..... $m^2 \cdot s^{-1}$
ν_T	eddy diffusivity of momentum ..... $m^2 \cdot s^{-1}$
ξ	dimensionless position of the interface, defined in Fig. 1
ρ_f	fluid density ..... $kg \cdot m^{-3}$
τ_i	shear stress at the porous/fluid interface $N \cdot m^{-2}$
ϕ	dimensionless temperature for the constant wall temperature case, $= (T - T_W)/(T_m - T_W)$

is shared by Nield [9] who, referencing a book by Bear [10], pointed out that actual turbulence occurs at values of the Reynolds number at least one order of magnitude higher than the Reynolds number at which the flow starts deviating from the Darcy law. The authors of this paper share Dr. Nield's point of view expressed in Ref. [9]. Therefore, by utilizing Forchheimer and dispersion terms in equations for the porous region, they do not attempt to model turbulence in the porous layer, they assume that the flow in the porous region is laminar. However, because of the large filtration velocity, especially in the vicinity of the porous/fluid interface, non-Darcian effects must be accounted for.

Fig. 1 displays a schematic diagram of the problem considered in this paper. It is assumed that the central portion of the circular tube, $0 \leqslant r \leqslant \xi R$, is occupied by a clear fluid while its peripheral part, $\xi R \leqslant r \leqslant R$, is occupied by an isotropic porous medium of uniform porosity. Two types of thermal boundary conditions at the tube wall are considered, a constant heat flux, q''_W, and a constant wall temperature, T_W. The entrance region is not considered, and the flow is assumed to be hydrodynamically and thermally fully developed.

2. Problem formulation

2.1. Governing equation in the porous region

Since the whole flow domain is divided into two regions, the central region which is occupied by a clear fluid (where the flow is turbulent) and the peripheral region occupied by a fluid saturated porous medium (where the flow is laminar), separate sets of governing equations must be formulated for each of these two regions. The solutions must then be matched at the porous/fluid interface.

For the porous region ($\xi R \leqslant r \leqslant R$), the Brinkman–Forchheimer extension of the Darcy law [7] is utilized. The Forchheimer term accounts for the deviation from linearity, which is essential for large filtration velocity. Brinkman

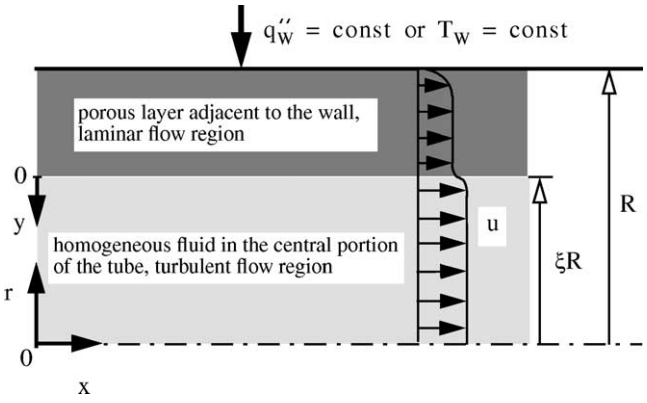

Fig. 1. Schematic diagram of the problem.

term allows retaining continuity of filtration velocity at the porous/fluid interface. Because of the turbulent flow in the central portion of the tube, it is convenient to introduce dimensionless variables similar to wall coordinates in turbulence modeling. These dimensionless coordinates are then used throughout the channel, in both laminar (porous) and turbulent (clear fluid) regions. For example, dimensionless radius is introduced as:

$$r^+ = u_\tau r/\nu_\mathrm{f} \tag{1}$$

where r is the dimensional radius; u_τ is the friction velocity at the porous/fluid interface; $(\tau_\mathrm{i}/\rho_\mathrm{f})^{1/2}$; ν_f is the fluid kinematic viscosity; ρ_f is the fluid density; and τ_i is the shear stress at the porous/fluid interface.

The dimensionless filtration velocity is defined as:

$$u^+ = u/u_\tau \tag{2}$$

where u is the dimensional filtration velocity (over the clear fluid region filtration velocity coincides with the fluid velocity).

In these dimensionless variables the Brinkman–Forchheimer-extended Darcy equation [7] can be presented as:

$$\frac{2}{\xi R^+} + \left(\frac{\mu_\mathrm{eff}}{\mu_\mathrm{f}}\right)\frac{1}{r^+}\frac{\mathrm{d}}{\mathrm{d}r^+}\left(r^+\frac{\mathrm{d}u^+}{\mathrm{d}r^+}\right) - \frac{u^+}{Da(R^+)^2} - \frac{c_\mathrm{F}}{Da^{1/2}R^+}\left(u^+\right)^2 = 0 \tag{3}$$

where c_F is the Forchheimer coefficient; Da is the Darcy number, K/R^2; R^+ is the dimensionless radius of the tube, $u_\tau R/\nu_\mathrm{f}$; μ_eff is the effective viscosity in the porous region; μ_f is the fluid dynamic viscosity; and ξ is the dimensionless position of the interface (cf. Fig. 1). The ratio $\mu_\mathrm{eff}/\mu_\mathrm{f}$ is a function of porosity of the porous medium. The porosity of the porous layer is assumed constant and uniform; therefore, the ratio $\mu_\mathrm{eff}/\mu_\mathrm{f}$ is also constant.

Eq. (3) is the momentum equation for the porous region. The energy equations for the porous region must be formulated separately for the constant wall heat flux and the constant wall temperature boundary conditions. For the *constant wall heat flux case* the dimensionless temperature can be defined as:

$$\theta = (1/Nu)(T - T_\mathrm{W})/(T_\mathrm{m} - T_\mathrm{W}) \tag{4}$$

where T is the temperature, T_W is the wall temperature (temperature at $r^+ = R^+$), T_m is the mean temperature in the tube:

$$T_\mathrm{m} = \frac{2}{R^2 U_\mathrm{m}}\int_0^R uTr\,\mathrm{d}r \tag{5}$$

U_m^+ is the mean fluid velocity in the tube:

$$U_\mathrm{m}^+ = \frac{2}{(R^+)^2}\int_0^{R^+} u^+ r^+\,\mathrm{d}r^+ \tag{6}$$

and Nu is the Nusselt number:

$$Nu = h2R/k_\mathrm{f} = 2Rq''_\mathrm{W}/\left[k_\mathrm{f}(T_\mathrm{W} - T_\mathrm{m})\right] \tag{7}$$

where h is the heat transfer coefficient and q''_W is the wall heat flux.

Assuming thermal equilibrium between the fluid and solid in the porous layer, the energy equation for the constant wall heat flux case can then be presented as:

$$\frac{1}{r^+}\frac{\mathrm{d}}{\mathrm{d}r^+}\left[\left(\frac{k_\mathrm{m}}{k_\mathrm{f}} + C\,Pr\,Re_\mathrm{p}u^+\right)r^+\frac{\mathrm{d}\theta}{\mathrm{d}r^+}\right] = -\frac{1}{(R^+)^2}\frac{u^+}{U_\mathrm{m}^+} \tag{8}$$

where C is dimensionless experimental constant in the correlation for thermal dispersion; k_f is the fluid thermal conductivity; k_m is the stagnant thermal conductivity of the porous medium (when $u^+ = 0$); Pr is the Prandtl number, $\nu_\mathrm{f}/a_\mathrm{f}$; a_f is the fluid thermal diffusivity; $Re_p = u_\tau d_\mathrm{p}/\nu_\mathrm{f}$ is the Reynolds number based on the average particle diameter, d_p, and the friction velocity at the porous/fluid interface, u_τ.

The term $C\,Pr\,Re_\mathrm{p}u^+$ in Eq. (8) accounts for the transverse thermal dispersion (Amiri and Vafai [11,12], Plumb [13]). Longitudinal thermal dispersion and longitudinal thermal conduction are neglected, which are valid assumptions if Peclet number is large.

For the *constant wall temperature case* the dimensionless temperature is redefined as:

$$\phi = \frac{T - T_\mathrm{W}}{T_\mathrm{m} - T_\mathrm{W}} \tag{9}$$

The dimensionless energy equation in the porous region for the constant wall temperature case is:

$$\frac{1}{r^+}\frac{\mathrm{d}}{\mathrm{d}r^+}\left[\left(\frac{k_\mathrm{m}}{k_\mathrm{f}} + C\,Pr\,Re_\mathrm{p}u^+\right)r^+\frac{\mathrm{d}\phi}{\mathrm{d}r^+}\right] = -\frac{1}{(R^+)^2}Nu\,\phi\frac{u^+}{U_\mathrm{m}^+} \tag{10}$$

2.2. Governing equation in the clear fluid region

To obtain the momentum equation for the clear fluid region a two-layer algebraic turbulence model suggested by Cebeci and Smith (Cebeci and Smith [14], Wilcox [15]) is utilized. According to this model, the velocity distribution in the clear fluid region, $0 \leqslant r \leqslant \xi R$, is computed from the following equation:

$$\frac{\mathrm{d}u^+}{\mathrm{d}y^+} = \frac{1}{1+\mu_{\mathrm{T}}^+}\left(1-\frac{y^+}{\xi R^+}\right) \tag{11}$$

where y^+ is the dimensionless distance from the porous/fluid interface, $\xi R^+ - r^+$; μ_{T}^+ is the dimensionless eddy viscosity, $\mu_{\mathrm{T}}/\mu_{\mathrm{f}}$; and μ_{T} is the eddy viscosity.

According to the Cebeci–Smith model [14,15], the turbulent flow domain is divided into two layers, the inner layer ($0 \leqslant y^+ \leqslant y_{\mathrm{m}}^+$) and the outer layer ($y^+ > y_{\mathrm{m}}^+$). The dimensionless eddy viscosity is then computed as:

$$\mu_{\mathrm{T}}^+ = \begin{cases} \mu_{\mathrm{T_i}}^+ & \text{for } y^+ \leqslant y_{\mathrm{m}}^+ \\ \mu_{\mathrm{T_o}}^+ & \text{for } y^+ > y_{\mathrm{m}}^+ \end{cases} \tag{12}$$

where y_{m}^+ is the smallest value of y^+ for which $\mu_{\mathrm{T_i}} = \mu_{\mathrm{T_o}}$. The value of the dimensionless eddy viscosity in the inner layer, $\mu_{\mathrm{T_i}}^+$, is computed according to the following equation:

$$\mu_{\mathrm{T_i}}^+ = \left(\kappa y^+\right)^2\left[1-\exp\left(-y^+/A^+\right)\right]^2\left|\mathrm{d}u^+/\mathrm{d}y^+\right| \tag{13}$$

and the value of the dimensionless eddy viscosity in the outer layer, $\mu_{\mathrm{T_o}}^+$, is computed as:

$$\mu_{\mathrm{T_o}}^+ = \alpha_{\mathrm{T}} U_{\mathrm{c}}^+ \delta_{\mathrm{v}}^+ F_{\mathrm{Kleb}} \tag{14}$$

where U_{c}^+ is the dimensionless centerline velocity, $(u|_{r=0})/u_\tau$; F_{Kleb} is the Klebanoff intermittency function:

$$F_{\mathrm{Kleb}} = \left[1+5.5\left[y^+/\left(\xi R^+\right)\right]^6\right]^{-1} \tag{15}$$

and δ_{v}^+ is the dimensionless velocity thickness:

$$\delta_{\mathrm{v}}^+ = \int_0^{\xi R^+} \left(1-u^+/U_{\mathrm{c}}^+\right)\mathrm{d}y^+ \tag{16}$$

The closure coefficients for the Cebeci–Smith model are:

$$\kappa = 0.40, \qquad \alpha_{\mathrm{T}} = 0.0168, \qquad A^+ = 26 \tag{17}$$

The energy equation for the clear fluid region is based on the constant turbulent Prandtl number model. For the *constant wall heat flux case* the energy equation can be presented as:

$$\frac{1}{r^+}\frac{\mathrm{d}}{\mathrm{d}r^+}\left[\left(1+\mu_{\mathrm{T}}^+\frac{Pr}{Pr_{\mathrm{t}}}\right)r^+\frac{\mathrm{d}\theta}{\mathrm{d}r^+}\right] = -\frac{1}{(R^+)^2}\frac{u^+}{U_{\mathrm{m}}^+} \tag{18}$$

where Pr_{t} is the turbulent Prandtl number, $\nu_{\mathrm{T}}/a_{\mathrm{T}}$; and a_{T} is the eddy diffusivity of heat.

For the *constant wall temperature case*, the energy equation is:

$$\frac{1}{r^+}\frac{\mathrm{d}}{\mathrm{d}r^+}\left[\left(1+\mu_{\mathrm{T}}^+\frac{Pr}{Pr_{\mathrm{t}}}\right)r^+\frac{\mathrm{d}\phi}{\mathrm{d}r^+}\right] = -\frac{1}{(R^+)^2}Nu\,\phi\frac{u^+}{U_{\mathrm{m}}^+} \tag{19}$$

2.3. Boundary conditions

Boundary conditions at the wall

At the wall of the tube the no-slip boundary condition is utilized:

$$u^+|_{r^+=R^+} = 0 \tag{20}$$

The utilization of no-slip boundary condition at the tube wall is possible because of the Brinkman term in the momentum equation for the porous region, Eq. (3).

In addition to this, the following thermal boundary condition is utilized at the tube wall for the *constant wall heat flux case*:

$$\theta|_{r^+=R^+} = 0 \tag{21}$$

A similar condition is utilized for the *constant wall temperature case*:

$$\phi|_{r^+=R^+} = 0 \tag{22}$$

Boundary conditions at the porous/fluid interface

From the definitions of u^+ and r^+ the following hydrodynamic boundary condition on the clear fluid side of the porous/fluid interface is obtained:

$$\left.\frac{\partial u^+}{\partial r^+}\right|_{r^+=\xi R^+-0} = -1 \tag{23}$$

In addition, the following matching hydrodynamic boundary conditions are utilized:

$$u^+|_{r^+=\xi R^+ +0} = u^+|_{r^+=\xi R^+-0} = u_{\mathrm{i}}^+ \tag{24}$$

and

$$\left(\frac{\mu_{\mathrm{eff}}}{\mu_{\mathrm{f}}}\right)\left.\frac{\partial u^+}{\partial r^+}\right|_{r^+=\xi R^+ +0} - \left.\frac{\partial u^+}{\partial r^+}\right|_{r^+=\xi R^+-0} = \frac{\beta u_{\mathrm{i}}^+}{Da^{1/2}R^+} \tag{25}$$

where u_{i}^+ is the dimensionless velocity at the porous/fluid interface, u_{i}/u_τ; and β is the dimensionless adjustable coefficient. Eq. (24) simply postulates the continuity of the filtration velocity across the interface. Eq. (25) is more interesting because it postulates a jump in the shear stress across the interface, the magnitude of this jump is proportional to the filtration velocity at the interface and the empirical coefficient β. These boundary conditions are derived utilizing complicated volume averaging procedure in Ochoa–Tapia and Whitaker [16,17]. The original derivation in [16,17] assumed laminar flow in both clear fluid and porous regions. However, according to the Cebeci–Smith model (Eq. (13)), the dimensionless eddy viscosity, μ_{T}^+, equals zero at the porous/fluid interface. Thus it is assumed that Eqs. (24) and (25) are still valid for the flow situation considered in this paper.

Finally, continuity of temperature and heat flux is assumed across the interface. This translates into the following equations for the *constant wall heat flux*

$$\theta|_{r^+=\xi R^+-0} = \theta|_{r^+=\xi R^+ +0} \tag{26a}$$

$$\left.\frac{\partial\theta}{\partial r^+}\right|_{r^+=\xi R^+-0} = \frac{k_{\text{eff}}}{k_{\text{f}}}\left.\frac{\partial\theta}{\partial r^+}\right|_{r^+=\xi R^+ +0} \tag{26b}$$

and the *constant wall temperature*

$$\phi|_{r^+=\xi R^+-0} = \phi|_{r^+=\xi R^+ +0} \tag{27a}$$

$$\left.\frac{\partial\phi}{\partial r^+}\right|_{r^+=\xi R^+-0} = \frac{k_{\text{eff}}}{k_{\text{f}}}\left.\frac{\partial\phi}{\partial r^+}\right|_{r^+=\xi R^+ +0} \tag{27b}$$

cases, respectively.

Boundary conditions in the center of the tube

No additional hydrodynamic boundary conditions are required for Eq. (11) because this is the first-order equation and, therefore, requires just one boundary condition, either at the porous/fluid interface or in the center of the tube. Since hydrodynamic boundary condition at the interface has already been formulated (cf. Eqs. (23)–(25)), no hydrodynamic boundary condition in the center is needed. It is also worth noting that the solution of Eq. (11) automatically satisfies the symmetry condition ($\partial u^+/\partial y^+ = 0$) in the center of the tube, at $y^+ = \xi R^+$.

For the energy equation, the following symmetry boundary condition is utilized. For the *constant wall heat flux case* this boundary condition is presented as:

$$\left.\frac{\partial\theta}{\partial r^+}\right|_{r^+=0} = 0 \tag{28}$$

Similarly, for the *constant wall temperature case*, this boundary condition is presented as:

$$\left.\frac{\partial\phi}{\partial r^+}\right|_{r^+=0} = 0 \tag{29}$$

2.4. Computation of the Nusselt number

The Nusselt number is computed utilizing the compatibility condition (Bejan [18]). For the *constant wall heat flux case* this condition is presented as:

$$Nu = U_{\text{m}}^+\left(R^+\right)^2 \Big/ \left[2\int_0^{R^+} u^+\theta r^+ \,\mathrm{d}r^+\right] \tag{30}$$

For the *constant wall temperature case* the appropriate compatibility condition is:

$$Nu = -2\frac{k_{\text{eff}}}{k_{\text{f}}}R^+\left.\frac{\mathrm{d}\phi}{\mathrm{d}r^+}\right|_{r^+=R^+} \tag{31}$$

3. Results and discussion

Governing equations are discretized utilizing the finite-difference method. The solution procedure is outlined in Wilcox [15]. The most important assumption made in this paper is that the flow in the porous layer is laminar while the flow in the clear fluid region is turbulent. The validity of this assumption can be easily estimated by comparing values of pertinent Reynolds numbers with their critical values. To check whether the flow in the clear fluid region is indeed turbulent it is necessary to calculate the Reynolds number based on the diameter of the clear fluid region, $2\xi R$, and the mean velocity in this region, $(U_{\text{m}})_{\text{clear fl}}$:

$$Re_{2\xi R} = (U_{\text{m}})_{\text{clear fl}}2\xi R/\nu_{\text{f}} = \left(U_{\text{m}}^+\right)_{\text{clear fl}}2\xi R^+ \tag{32}$$

where $(U_{\text{m}}^+)_{\text{clear fl}}$ is the dimensionless mean velocity in the clear fluid region, which is defined as:

$$\left(U_{\text{m}}^+\right)_{\text{clear fl}} = \frac{2}{(\xi R^+)^2}\int_0^{\xi R^+} u^+ r^+ \,\mathrm{d}r^+ \tag{33}$$

As shown in Ref. [19] (thermal dispersion in the porous layer is neglected in this reference, however, because temperature dependence of viscosity is also neglected, this does not influence the hydrodynamic solution), for $R^+ = 1000$, $Da = 10^{-4}$, and $\xi = 0.6$ the value of $Re_{2\xi R}$ is 8.928×10^3, which is larger than the critical Reynolds number of 4×10^3. This means that the flow in the clear fluid region is turbulent.

To check whether the flow in the porous layer remains laminar the Reynolds number based on $K^{1/2}$ must be estimated:

$$Re_{\text{K}} = v_{\text{fil}}K^{1/2}/\nu_{\text{f}} \tag{34}$$

where K is the permeability of the porous medium.

Estimating filtration velocity, v_{fil}, in the bulk of the fluid region gives that for $R^+ = 1000$, $Da = 10^{-4}$, and $\xi = 0.6$, Re_{K} is equal to 1.715, which is much smaller than the critical value of 100, which means that the flow in the porous region is laminar. (The value of 100 is an estimate; it follows from Refs. [7,10] and should be considered as a lower limit of the critical value of Re_{K} for porous media, the actual critical value of Re_{K} may be larger.)

Values of all parameters utilized in computations are shown directly in the figures. The large value of Re_p is utilized to show the effect of thermal dispersion. Fig. 2(a) depicts dimensionless velocity profiles for different values of the Darcy number. A larger value of the Darcy number corresponds to larger permeability; therefore, velocity in the porous region is larger for larger value of Da. It is interesting, however, that the flow velocity in the clear fluid region exhibits significant dependence on the Darcy number as well. This is because the Darcy number influences the velocity at the porous/fluid interface, u_{i}^+, which serves as a "starting point" for the turbulent velocity profile.

Fig. 2(b) and (c) display distributions of the dimensionless temperature for constant wall heat flux and constant wall temperature cases, respectively. Variation of the Darcy number has considerable impact on the temperature profiles. This is because convection is responsible for the major part of heat transfer from the wall, and the variation of the velocity distribution that occurs because of the variation of the Darcy number impacts the temperature distribution as well.

Fig. 3 displays the dependence of the Nusselt number on the dimensionless experimental constant in the correla-

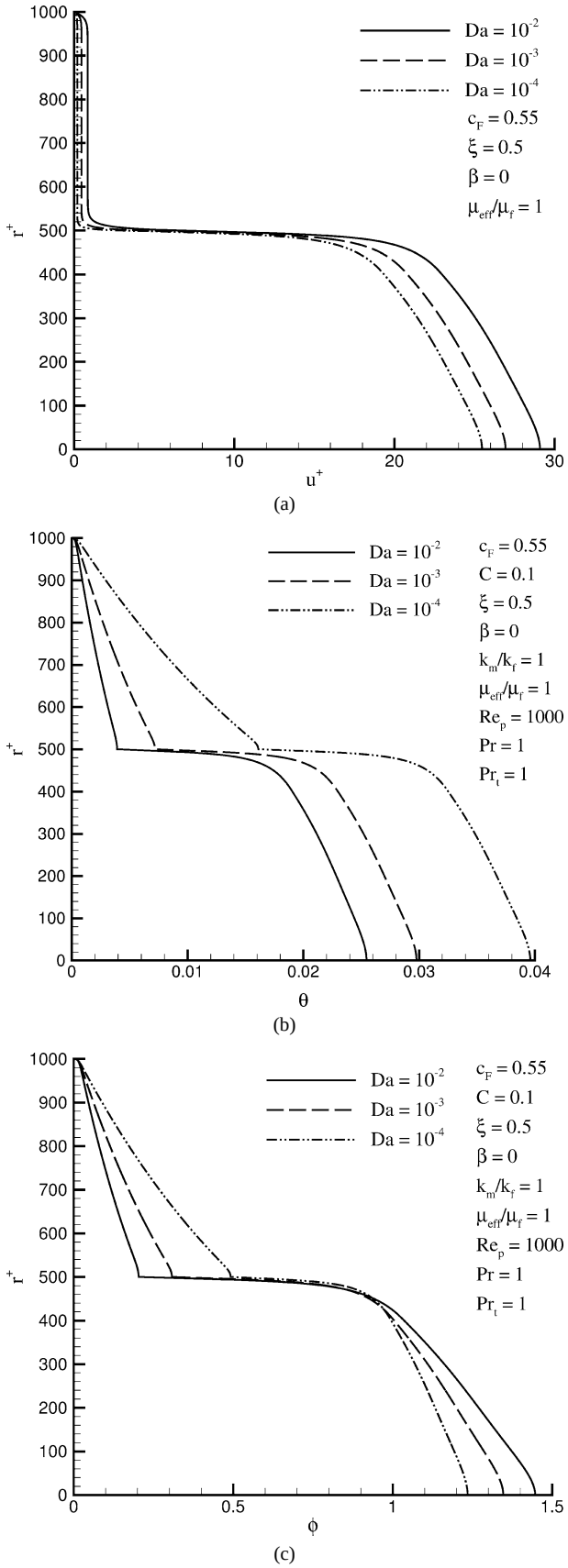

Fig. 2. Dimensionless velocities (a) and dimensionless temperatures for the isoflux (b) and isothermal (c) wall for different values of the Darcy number assuming turbulent flow in the central portion of the tube.

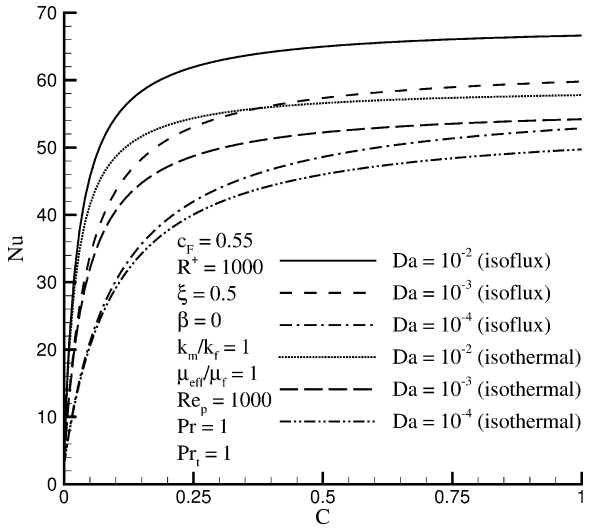

Fig. 3. Dependence of the Nusselt number on the dimensionless experimental constant in the correlation for thermal dispersion, C, for different values of the Darcy number for isoflux and isothermal walls.

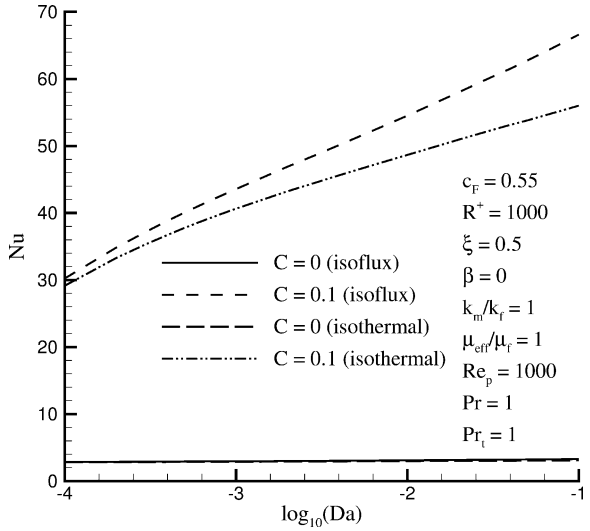

Fig. 4. Dependence of the Nusselt number on the Darcy number for isoflux and isothermal walls accounting for thermal dispersion ($C = 0.1$) and neglecting it ($C = 0$).

tion for thermal dispersion. This figure illuminates the effect of thermal dispersion on the Nusselt number. Thermal dispersion leads the apparent increase of effective thermal conductivity of the porous medium because of the hydrodynamic mixing of the interstitial fluid at the pore scale. Since thermal dispersion increases apparent thermal conductivity of the porous medium, it also increases the Nusselt number. This increase is especially fast for small values of C. As C increases, the slope of the curve becomes closer to horizontal. This means that the curve approaches its asymptotic limit that physically corresponds to the situation when thermal conductivity of the porous layer is infinitely large. In this case the value of the Nusselt number is determined by heat transfer in the clear fluid core of the tube alone.

Fig. 4 displays the effect of the Dacry number on the Nusselt number for two cases, when thermal dispersion is accounted for ($C = 0.1$, this value of C for transverse thermal dispersion follows from experimental data of Wakao and Kaguei [20]) and neglected ($C = 0$). This figure shows that the Darcy number has significant effect on the Nusselt number when thermal dispersion is accounted for. However, it has very little effect when thermal dispersion is neglected. This is because accounting for thermal dispersion results in heavy dependence of effective thermal conductivity of the porous medium on the flow velocity. The flow velocity in the porous region is controlled by permeability, that is, by the Darcy number.

4. Conclusions

In this paper, an engineering approach toward computations of turbulent flows in composite porous/fluid domains is suggested. This approach is based on the assumption that although the flow in the clear fluid region is turbulent, the flow in the porous region remains laminar. The whole porous domain is thus approximated as a laminar sublayer. It is expected that this approach will perform well for porous media of small permeability, because the penetration depth of turbulent eddies coming from the clear fluid region into this media is very small. Further experimental research to validate this approach is needed.

Acknowledgements

The authors acknowledge with gratitude the assistance of the North Carolina Supercomputing Center (NCSC) under an Advanced Computing Resources Grant.

References

[1] H. Wang, E.S. Takle, Boundary-layer flow and turbulence near porous obstacles, Boundary Layer Meteorol. 74 (1995) 73–88.
[2] P.J. Prescott, F.P. Incropera, The effect of turbulence on solidification of a binary metal alloy with electromagnetic stirring, ASME J. Heat Transfer 117 (1995) 716–724.
[3] S.Y. Kim, J.-M. Koo, A.V. Kuznetsov, Effect of anisotropy in permeability and effective thermal conductivity on thermal performance of an aluminum foam heat sink, Numer. Heat Transfer A 40 (2001) 21–36.
[4] B.V. Antohe, J.L. Lage, A general two-equation macroscopic model for incompressible flow in porous media, Internat. J. Heat Mass Transfer 40 (1997) 3013–3024.
[5] M. Prakash, O.F. Turan, Y.G. Li, J. Mahoney, G.R. Thorpe, Impinging round jet studies in a cylindrical enclosure with and without a porous layer: Part I—Flow visualizations and simulations, Chem. Engrg. Sci. 56 (2001) 3855–3878.
[6] M. Prakash, O.F. Turan, Y.G. Li, J. Mahoney, G.R. Thorpe, Impinging round jet studies in a cylindrical enclosure with and without a porous layer: Part II—LDV measurements and simulations, Chem. Engrg. Sci. 56 (2001) 3879–3892.
[7] D.A. Nield, A. Bejan, Convection in Porous Media, 2nd Edition, Springer, New York, 1999.
[8] T. Masuoka, Y. Takatsu, Turbulence model for flow through porous media, Internat. J. Heat Mass Transfer 39 (1996) 2803–2809.
[9] D.A. Nield, Turbulence model for flow through porous media—Comments, Internat. J. Heat Mass Transfer 40 (1997) 2499–2499.
[10] J. Bear, Dynamics of Fluids in Porous Media, Elsevier, New York, 1972 (corrected reprint, Dover, New York, 1988).
[11] A. Amiri, K. Vafai, Transient analysis of incompressible flow through a packed bed, Internat. J. Heat Mass Transfer 41 (1998) 4259–4279.
[12] A. Amiri, K. Vafai, Analysis of dispersion effects and non-thermal equilibrium, non-Darcian, variable porosity incompressible flow through porous media, Internat. J. Heat Mass Transfer 37 (1994) 939–954.
[13] O.A. Plumb, The effect of thermal dispersion on heat transfer in packed bed boundary layers, in: Proceedings of ASME JSME Thermal Engineering Joint Conference, Vol. 2, 1983, pp. 17–22.
[14] T. Cebeci, A.M.O. Smith, Analysis of Turbulent Boundary Layers, in: Ser. in Appl. Math. Mech., Vol. 15, Academic Press, New York, 1974.
[15] D.C. Wilcox, Turbulence Modeling for CFD, DCW Industries, La Canada, CA, 1994.
[16] J.A. Ochoa-Tapia, S. Whitaker, Momentum transfer at the boundary between a porous medium and a homogeneous fluid—I. Theoretical development, Internat. J. Heat Mass Transfer 38 (1995) 2635–2646.
[17] J.A. Ochoa-Tapia, S. Whitaker, Momentum transfer at the boundary between a porous medium and a homogeneous fluid—II. Comparison with experiment, Internat. J. Heat Mass Transfer 38 (1995) 2647–2655.
[18] A. Bejan, Heat Transfer, Wiley, New York, 1993.
[19] A.V. Kuznetsov, L. Cheng, M. Xiong, Investigation of turbulence effects on forced convection in a composite porous/fluid duct: Constant wall flux and constant wall temperature cases, Heat Mass Transfer, in press.
[20] N. Wakao, S. Kaguei, Heat and Mass Transfer in Packed Beds, Gordon and Breach, New York, 1982.